ISSN 0915-[illegible]

JP9955269

NATIONAL INSTITUTE FOR FUSION SCIENCE

Analysis of Visisble Spectral Lines in LHD Helium Discharge

B.N. Wan, M. Goto and S. Morita

(Received - May 13, 1999)

NIFS-TECH-7 June 1999

30 - 50 D

This report was prepared as a preprint of work performed as a collaboration reserch of the National Institute for Fusion Science (NIFS) of Japan. This document is intended for infomation only and for future publication in a journal after some rearrangements of its contents.

Inquiries about copyright and reproduction should be addressed to the Research Information Center, National Institute for Fusion Science, Oroshi-cho, Toki-shi, Gifu-ken 509-5292 Japan.

Analysis of visible spectral lines in LHD helium discharge

B. N. Wan*, M. Goto and S. Morita
National Institute for Fusion Science, Toki, Japan
* *Institute of Plasma Physics, Chinese Academy of Science, Hefei, China*

Abstract

In this study, visible spectral lines in LHD helium discharges are analyzed and it was found that they could be well fitted with gaussian profile. The results reveal a simple mechanism of of helium atom recycling. Ion temperatures were also derived from the fitting. A typical value of the ion temperature obtained was about 6 eV.

Keywords: hydrogen, helium, space distribution profile, Doppler broadening, Doppler shift, double gaussian profile

I. Introduction

Understanding the behavior of neutral particle at edge region in fusion plasmas is necessary to control fuelling and recycling. The spectral profile of neutral particle emission lines (H_α, D_α, He I, ...) from edge plasma contains information on the velocity distribution of neutral particles and their basic recycling processes. The velocity distribution of the atoms determines their penetration depth into plasmas. Knowledge of atomic and molecular processes, which can be studied from emission spectra of neutral particles, is an important issue to understand mechanisms of edge recycling.

In HT-6M, H_α lines in front of limiter have been observed with high-resolution spectrometer and analyzed by fitting spectral line shape with multi-gaussian profiles and deriving velocity distribution of neutral hydrogen atoms [1]. Contributions of atomic, molecular and reflection processes in H_α line can be identified. Monte-Carlo simulation reproduces the spatial distribution of neutral hydrogen atoms measured by multi- channel H_α line monitoring. In TEXTOR, the profiles of H_α lines with and without CH_4 gas puffing have been investigated using high-resolution spectrometers[2], and contribution of molecular process (chemical sputtering) in edge recycling has been studied. In the TFTR DT-experiments the T_α line has recently been observed in the study of recycling and isotope exchange.

For spectral lines dominated with Doppler broadening, the ion temperature and flow velocity can be derived from spectral width and shift. In LHD, He I and H_α lines are observed from parallel multi-line of sight in helium discharges. A basic behavior of neutral particles at edge is investigated by spectral line analysis.

II. Experiments

The visible spectral profile of emission line was measured with a high-resolution spectrometer. Visible light emitted from LHD plasma is collected by lens and transferred through optical fibers to a diagnostic room. The optical fibers are coupled to the entrance slit of the spectrometer with CCD. The line of sight for the present study is vertically arranged from Z=−598 mm to Z=598 mm with 12 optical fibers. The 12 lines of sight are indicated with magnetic configuration in Fig. 1. The spectrometer is equipped with a CCD camera as a detector to measure spectra with spatial resolution. The absolute wavelength and spectral dispersion on CCD are determined from well-known emission lines. Figure 2b shows a spectrum in the LHD helium discharge. Three lines shown in the figure are He I at 6678.151 Å, H_α at 6562.793 Å and He I at 6560.099 Å respectively. The dispersion of the spectrometer on the CCD camera is determined to be −0.2297 Å/pix as shown in Fig. 2a. The instrumental width of the spectra on the CCD camera is estimated to be 3.5 pixels by measuring emission lines of Hg lamp.

The spectra of emission lines are integrated for 0.1 s. The present CCD camera has a periodical noise (Fig. 3b), which overlaps the spectra shown in Fig. 3a (it can be drastically reduced by cooling the CCD below −40°C). The noise can be subtracted by no-exposed signal (Fig. 3b) because the noise is stationary shown in Fig. 3c. To process the data, we can fit the pre-processed signal as shown in Fig. 3c. We can also fit raw data directly, where noise is treated as a polynomial background in the fitting procedure. Figure 4 shows the two fitting procedures. They give the same results, as an example for He I line at 6678.151 Å shown in Table 1.

Table I: Gaussian fitting for He I at 6678.151 Å.

Fit	height	center	FWHM
Sub. BKG	7395 ±37	35.6416 ±0.0088	3.8776 ±0.0207
Fit. BKG	7437 ±40	35.6412 ±0.0103	3.9148 ±0.0217

III. Spectral analysis

There are principally three spectral profiles, i.e. Gaussian-, Lorentzian- and Voigt profiles. Gaussian- and Lorentzian- profiles correspond to Doppler and pressure broadening mechanisms. Voigt profile is a mixture of Gaussian- and Lorentz-profiles. In fusion plasma, Doppler broadening is normally dominant. However, the pressure broadening may play an important role in line shape if we looked at a pellet ablation cloud or gas puffing. Therefore, it is necessary to check the line shape before analysis. Figure 5 gives the He I line at 5876 Å fitted by three spectral profiles and their residuals after fitting. The residual in Lorentz profile fitting has systematic distribution. Gaussian- and Voigt- profiles give a good fitting where their residuals show only statistic noise. In Voigt profile fitting, the shape parameter, which zero and one represent pure Gaussian- and Lorentzian-profiles, respectively, is only 0.06. This means Doppler broadening is dominant in spectral profile in present study. This result is reasonable because line of sight does not across the region of gas puffing. There is also no pellet injection in these shots we studied.

To investigate recycling at the edge, it is necessary to check the line shape by multi-gaussian fitting. The double gaussian profiles give the best and reproducible fitting to neutral helium emission lines at 6678 Å and 5876 Å. Otherwise, fitting with more than two gaussian profiles are not repeatable. This means that there exist mainly two gaussian profiles in measured helium emission lines. It should not be surprised because the neutral helium exists as atom. There is no molecular process involved in plasma at the edge. Possible contributions to He I emission lines are excitation of helium atom by electron impact, reflection at the surface of wall in the divertor region (see Fig. 1) and charge exchange. Typical double Gaussian fitting is shown in Fig. 6. The first one has narrow FWHM of 3.6 pixels and 91% area of the spectral line. It is due to radiation of helium atom excited by electron impact. The FWHM of spectral line in this part varies between 3.6–4.5 pixels for different lines of sight in many shots. This is only a little larger than instrumental width meaning a very low ion temperature. These results mean that most of neutral helium atom localize in a small region near the edge. The second gaussian profile has broader FWHM of 5.7 pixels and $\sim 9\%$ of area. The peak center is shifted upwards 1.6 pixels from peak center of the first one, corresponding to a wavelength downshift of 0.5 Å. We analyzed several tens of neutral helium lines in different shots. The summarized result shows values of FWHM (5.2–7.2 pixels), area (7–10%) and wavelength downshift (0.29–0.5 Å). This behavior of the second gaussian profile suggests a weak dependence on the main plasma. A possible contribution may be particle reflection from the wall. The reflected particle energy is estimated from wavelength shift and the value is about 1 eV.

In the following analysis, we fit emission lines only with a single gaussian profile to get intensity and rotation velocity because the second gaussian profile contributes spectral line less than 10%. The single gaussian fitting is shown in Fig. 4a and gives a good result with low and statistic residual. Figure 7 shows intensity and rotation velocity derived from Doppler shift of spectral line peak for He I line at 6678 Å in the LHD 6741 shot (last 100 ms). The channel 1 at Z=598.75 mm is far from plasma and does not have enough emission. Lines of sight of channel 11 at Z=−520.75 mm and channel 12 at −598.75 mm are also out of plasma. Signal of channel 12 is very weak and immerses in noise. Signal of channel 11 can be clearly seen. They may be caused by light reflection at the wall of vacuum vessel. The intensity profile of He I line is seemed to be broad. However, the penetration of neutral helium atom should not be deep into the plasma in LHD plasma parameters. It is possibly caused by a large contribution of recombination emission during quench of plasma, when the electron temperature may become very low. This behavior of helium atoms is checked by measuring another emission line of He I at 5876 Å. The result is shown in Fig. 8 in the LHD 6756 shot. The performance of this shot is very low as shown in Fig. 9. The maximum stored energy is only 32 kJ. A time evolution of He I emission intensity profile is shown in Fig. 10 for the LHD 6750 shot, whose performance is higher as shown in Fig. 11. The stored energy up to 127 kJ is achieved. The intensity of the emission line on the upper half plasma is higher than on lower half. It may be a result of trianglarity of the plasma, whose line of sight is longer on the upper half region as shown in Fig. 1. It is really difficult to derive the local profile of emission intensity because of contribution from the region outside LCFS.

The rotation of particle is seemed to be rigid. It may be a result of instrumental error, i.e. misalignment of optical fiber array against the detector. The FWHM of the spectral line from different channels varies very little as shown in Fig. 12, which supports the conclusion of narrow shell for distribution of neutral helium atoms. The ion temperature must be very low because the FWHM is only a little higher than instrumental width, which means concentration of helium atoms near the edge.

Behavior of helium ions is very similar to neutral helium atoms. The spectral result obtained from He II line at 4686 Å for the LHD 6747 shot is shown in Fig. 13. The performance of this shot is the same as the shot of 6750 as shown in Fig. 11. Only the FWHM of the spectral line is higher. The almost constant FWHM of the chord integrated spectral lines means the emission from a narrow region near the edge. Ion temperature is derived to be $\sim$ 6 eV higher than that derived from He I line. It is because helium ion has higher ionization potential and penetrates deeper into the plasma. The line integrated intensity profile of He II emission is shown in Fig. 14 and has similar behavior as He I emission.

IV. Discussion

An H_α line has been also observed in the present study. The neutral hydrogen particles are released from the wall due to exchange process with helium particles. However, the signal to noise ratio is not high enough to investigate recycling and particle exchange mechanisms. This topic is interesting to understand mechanisms in wall conditioning with helium discharge. For this purpose, more sensitive and less noise detection system is required.

The helium particles exist as single atoms. It has also a very low absorption by the wall of vacuum vessel. The mechanisms of recycling for helium become simple. In this study, a unique possible process is particle reflection at the wall. But its contribution may be very small. The emission from region outside LCFS causes this conclusion not very sure. A better configuration for this study is necessary to measure spectra with other line of sight to avoid this contribution. Of course, analysis in this study is also suitable to investigate divertor plasma in a special configuration to avoid emission from main plasma. It is really difficult to derive the local profile of emission intensity because of complicated magnetic configuration and contribution from region outside LCFS. But narrow distributions of helium atom and ion can still be determined from behaviors of spectral line. It is valuable to study the neutral hydrogen behavior by measuring H_α line in hydrogen discharge. Comparison of their behaviors can get new insight into the mechanisms of recycling at the edge.

In summary, a spectral line emitted from helium particle is analyzed in LHD helium discharges. A possible mechanism of recycling of helium atoms at edge is the reflection at the wall. But the ratio is very low. an ion temperature derived from emission line of helium ions is about 6 eV.

References

[1] B. N. Wan et al., IAEA-F1-CN69/EXP1/02, Yokohama(1998).

[2] U. Samm et al., Plasma Phys. Control. Fusion, **29**, 1321(1987).

[3] C. H. Skinner et al., J. Nucl. Mater. **241–243**, 887(1997).

Figure captions

FIG. 1 Magnetic configuration and lines of sight for spectral measurements.

FIG. 2 Calibration of wavelength and dispersion on CCD camera.

FIG. 3 Periodical noise (b) overlap on signal (a). It can be subtracted(c).

FIG. 4 Fitting data subtracted BKG (a) and including BKG.

FIG. 5 Spectral line fitting by Gaussian-, Lorentz- and Voigt profiles.

FIG. 6 . Double-gaussian profiles fitting for HeI line at 5876 A.

FIG. 7 Intensity and rotation velocity derived from HeI at 667.8nm in LHD 6741 shot.

FIG. 8 Line integrated intensity profile derived from HeI at 587.6nm in LHD 6756 shot.

FIG. 9 Elementary waveforms of LHD 6756 shot.

FIG. 10 Time evolution of line integrated emission in LHD 6750 shot for HeI at 587.6 nm.

FIG. 11 Elementary waveforms of LHD 6750 shot.

FIG. 12 FWHM of HeI at 587.6nm in LHD 6750 shot.

FIG. 13 Behavior of HeII line at 468.6nm. in LHD 6747 shot.

FIG. 14 Time evolution of line integrated emission in LHD 6747 shot for HeII at 468.6nm.

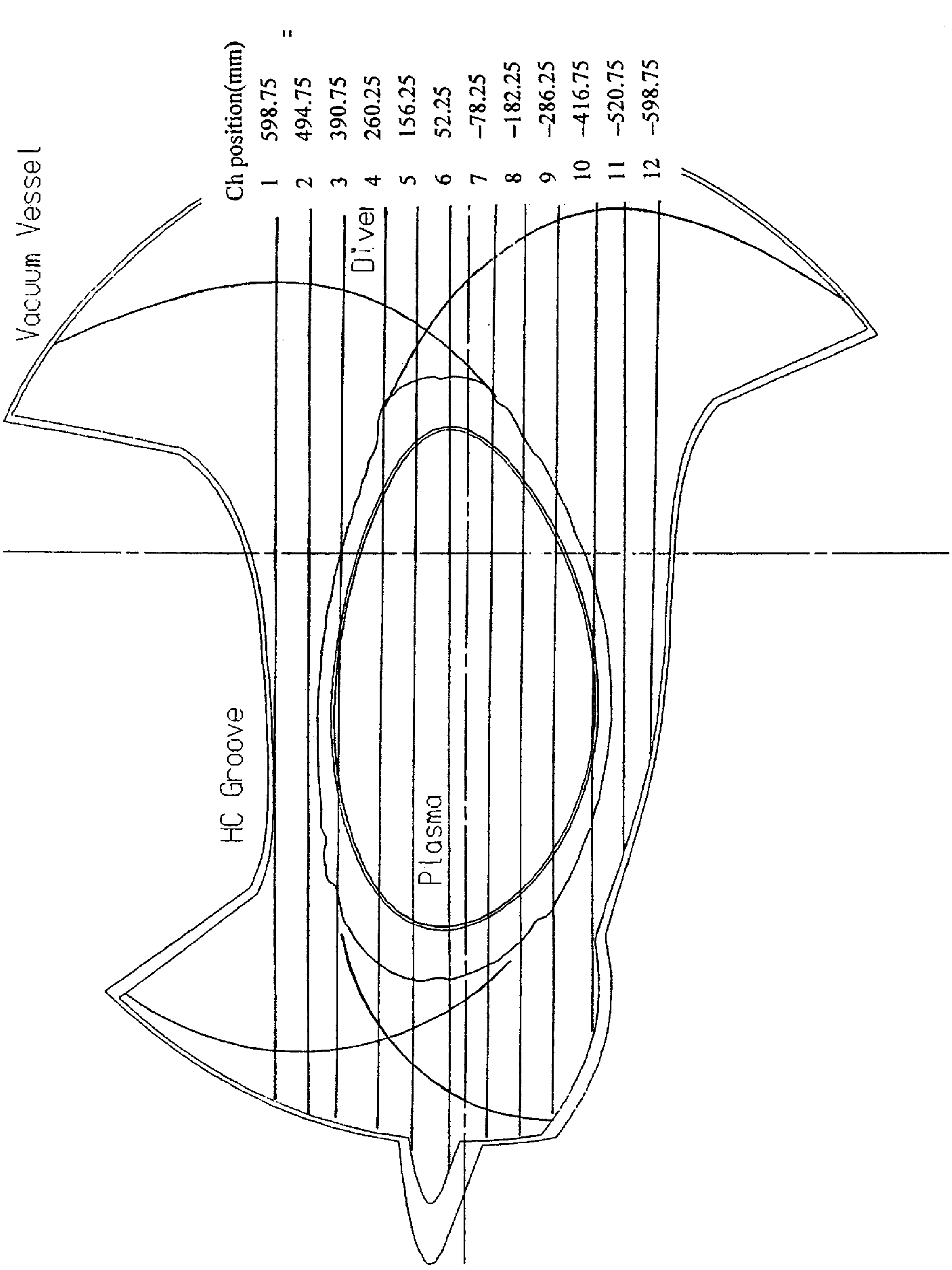
Vacuum Vessel
Ch position(mm)
1 598.75
2 494.75
3 390.75
4 260.25
5 156.25
6 52.25
7 -78.25
8 -182.25
9 -286.25
10 -416.75
11 -520.75
12 -598.75
Diver
HC Groove
Plasma

FIG. 1

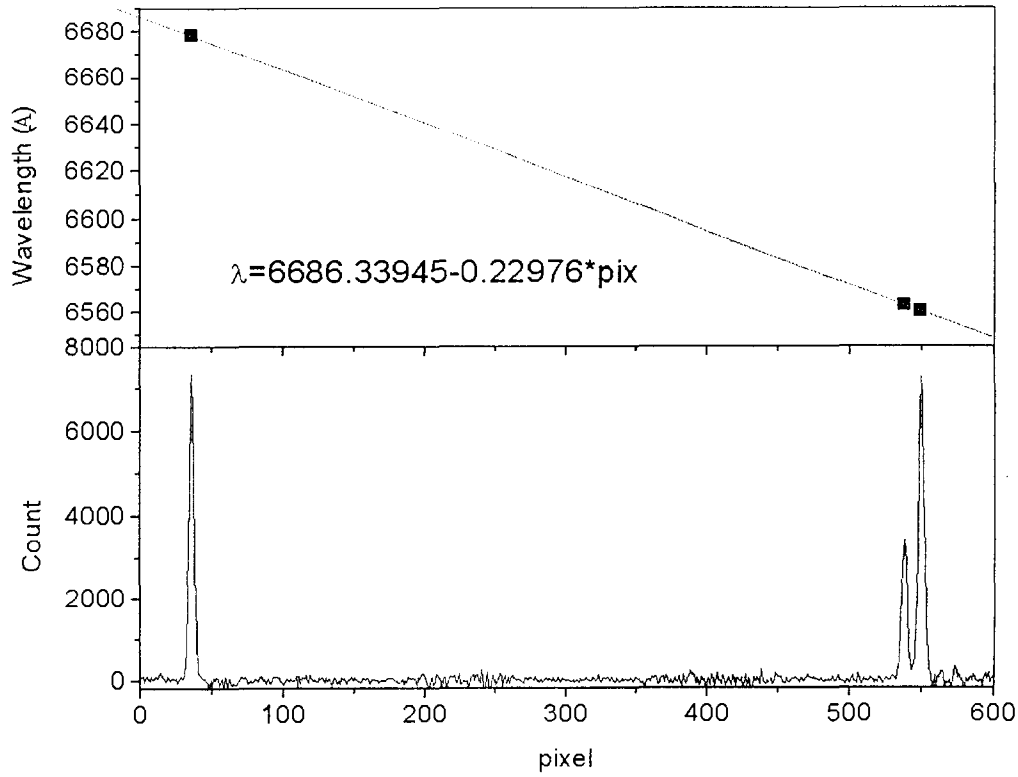
Wavelength (A)
λ=6686.33945-0.22976*pix
Count
pixel

FIG. 2

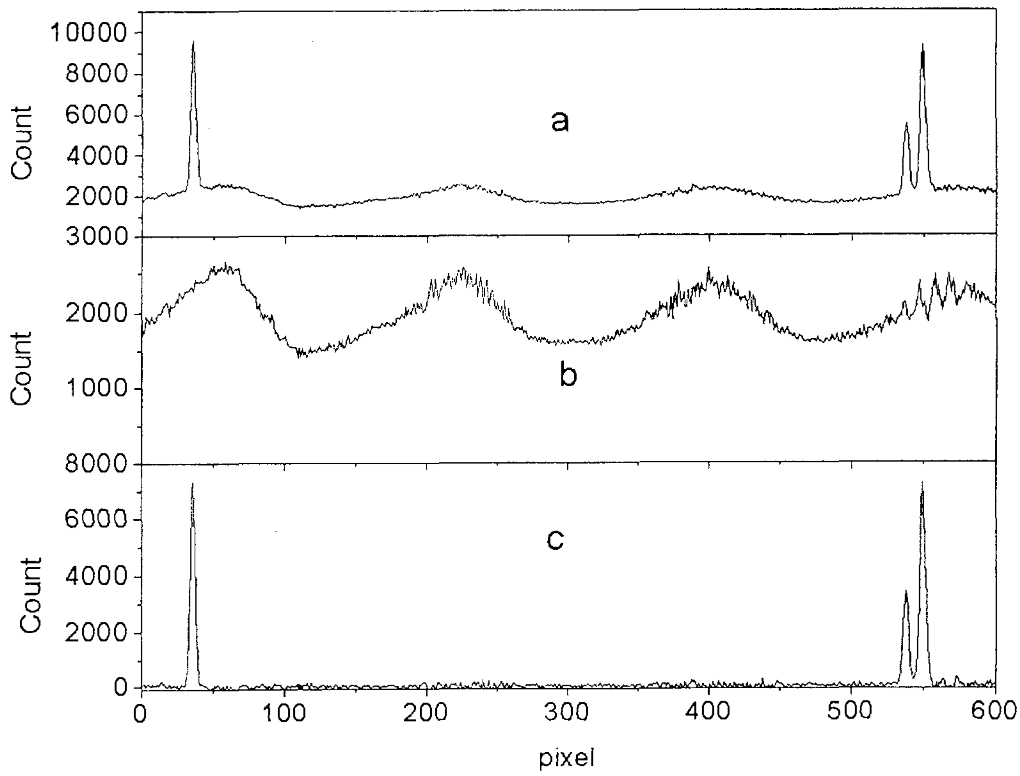
Count
a
b
c
pixel

FIG. 3

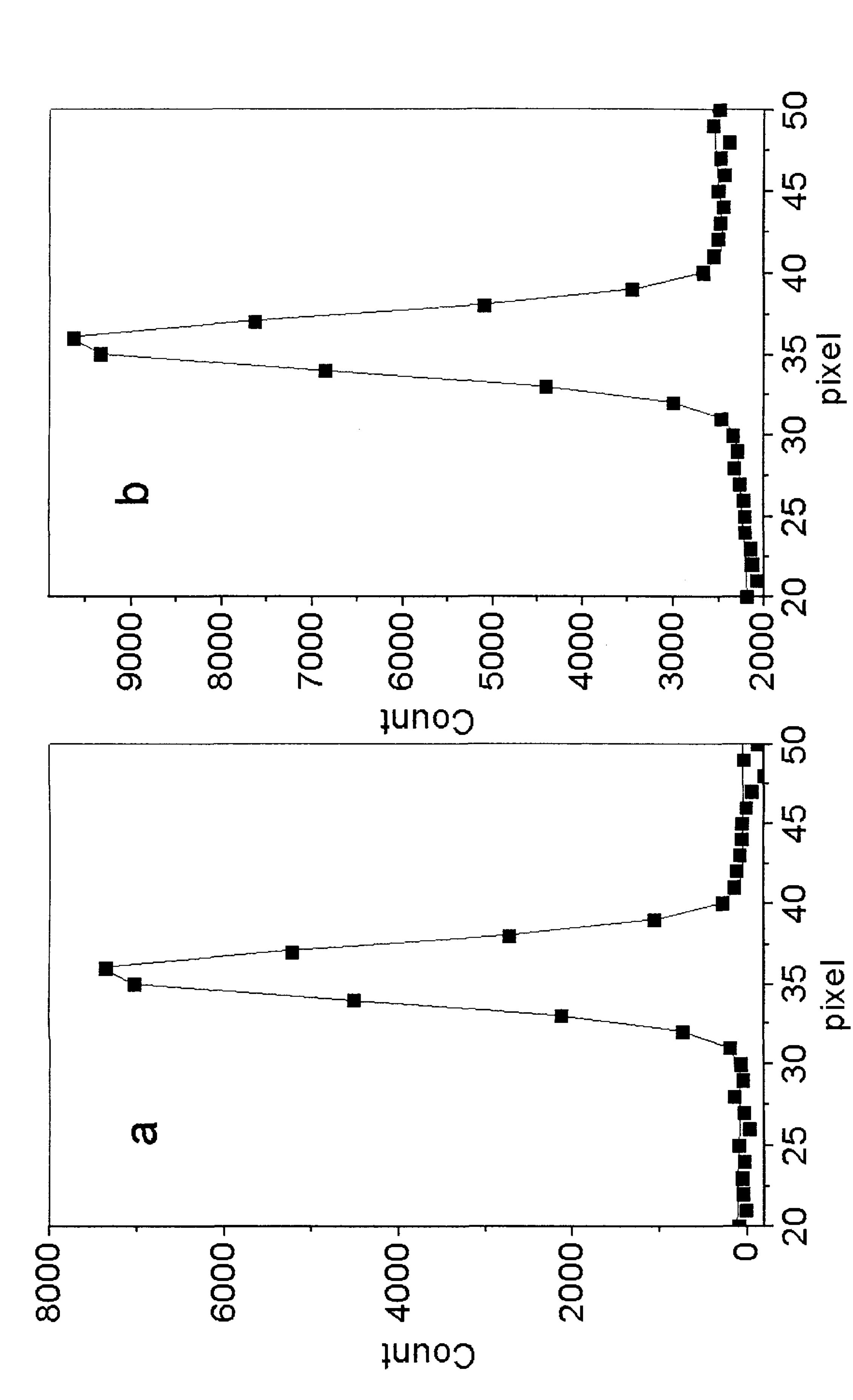

a
b
Count
pixel
8000
6000
4000
2000
0
9000
7000
5000
3000
20
25
30
35
40
45
50

FIG. 4

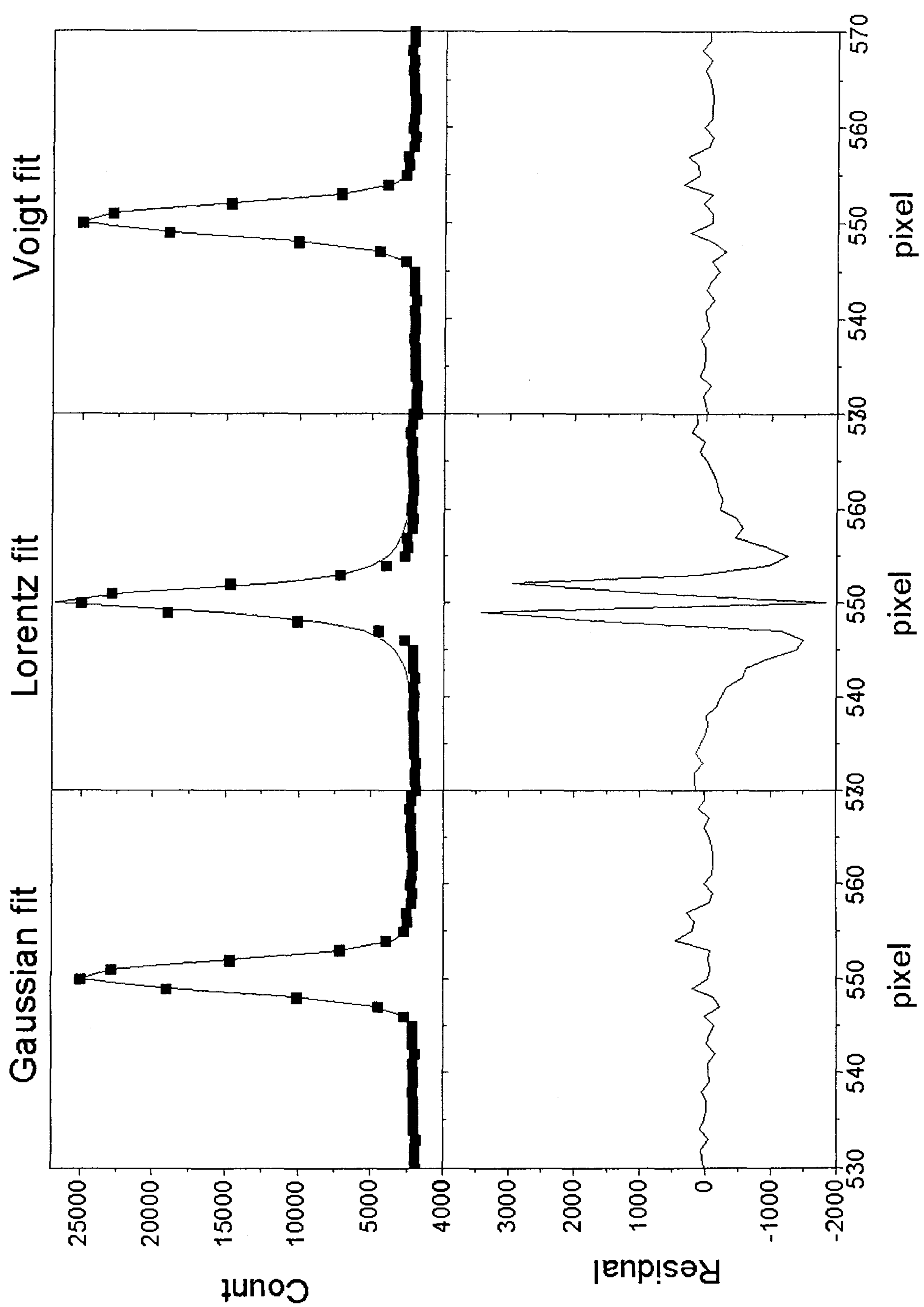
Gaussian fit
Lorentz fit
Voigt fit
Count
Residual
pixel
pixel
pixel
25000
20000
15000
10000
5000
4000
3000
2000
1000
0
-1000
-2000
530
540
550
560
570

FIG. 5

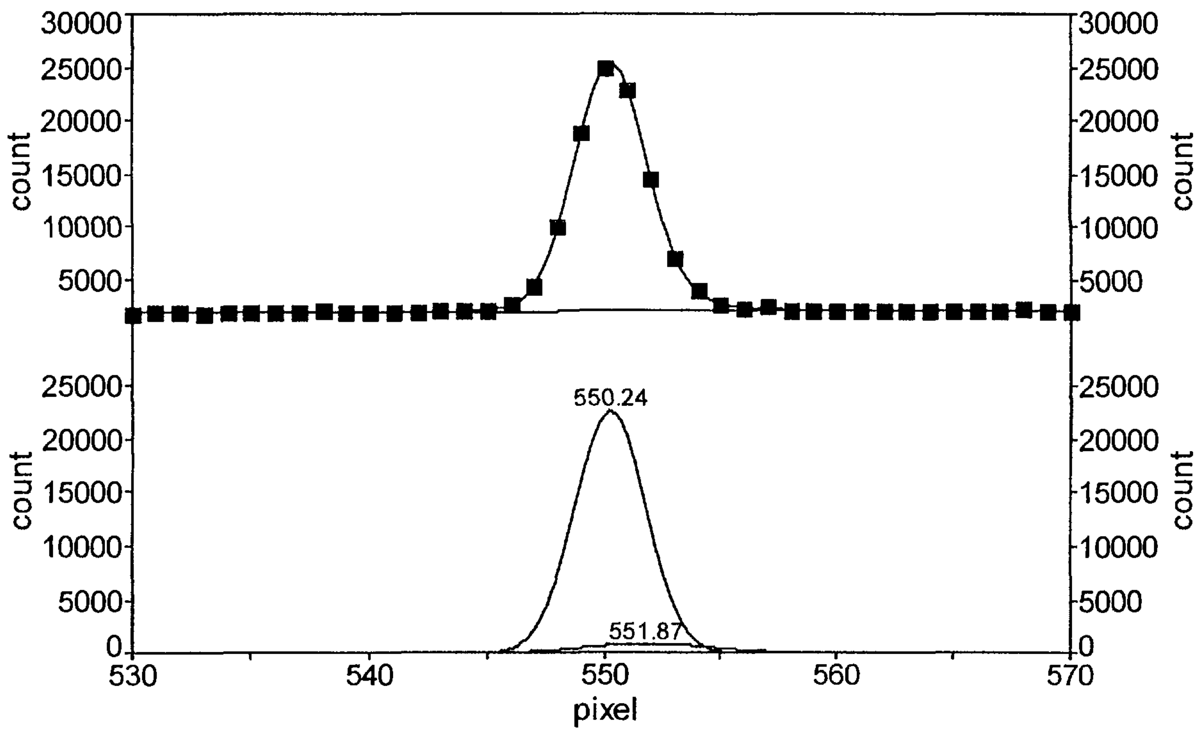
30000
25000
20000
15000
10000
5000
count
550.24
551.87
0
530
540
550
560
570
pixel

FIG. 6

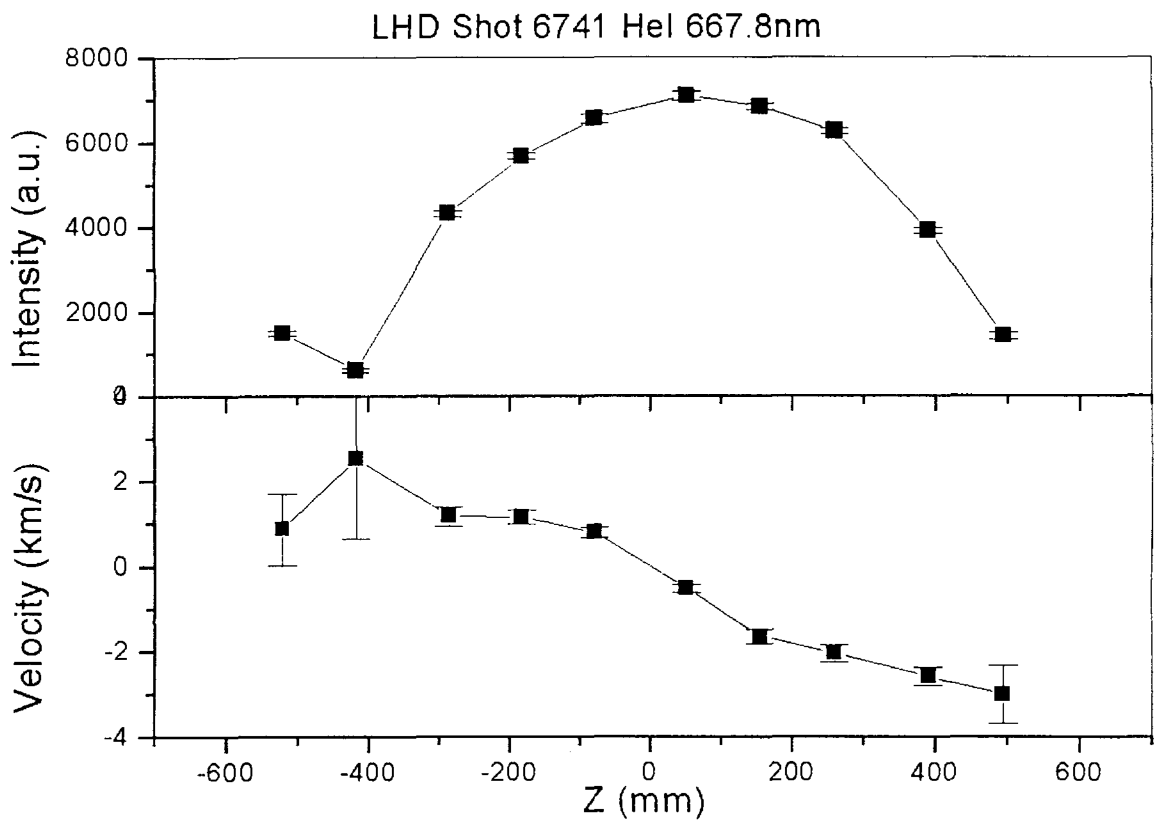
LHD Shot 6741 HeI 667.8nm
8000
6000
4000
2000
Intensity (a.u.)
Velocity (km/s)
2
0
-2
-4
-600
-400
-200
0
200
400
600
Z (mm)

FIG. 7

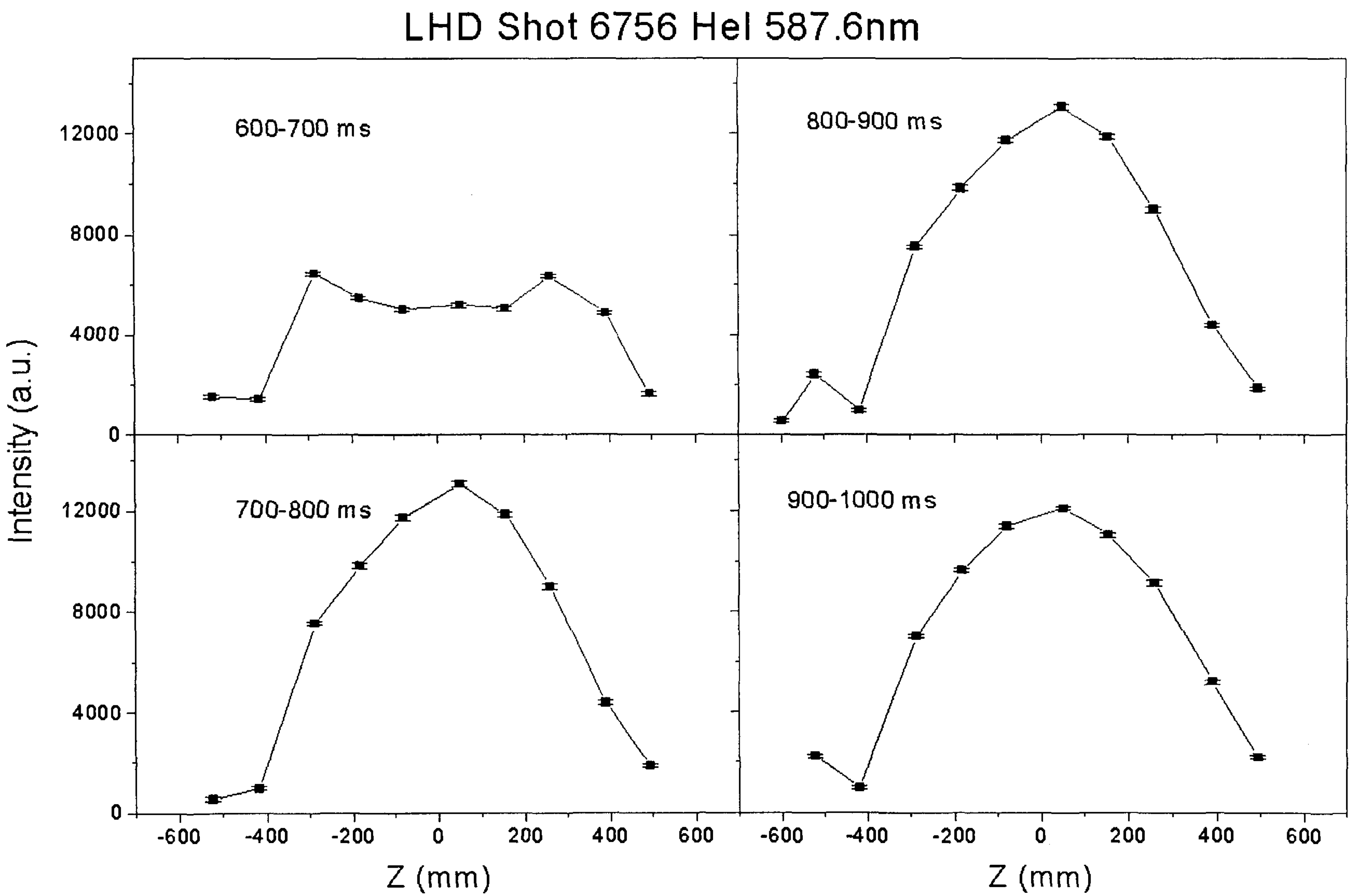
LHD Shot 6756 HeI 587.6nm
600-700 ms
800-900 ms
700-800 ms
900-1000 ms
Intensity (a.u.)
Z (mm)
Z (mm)
0
4000
8000
12000
-600
-400
-200
0
200
400
600

FIG. 8

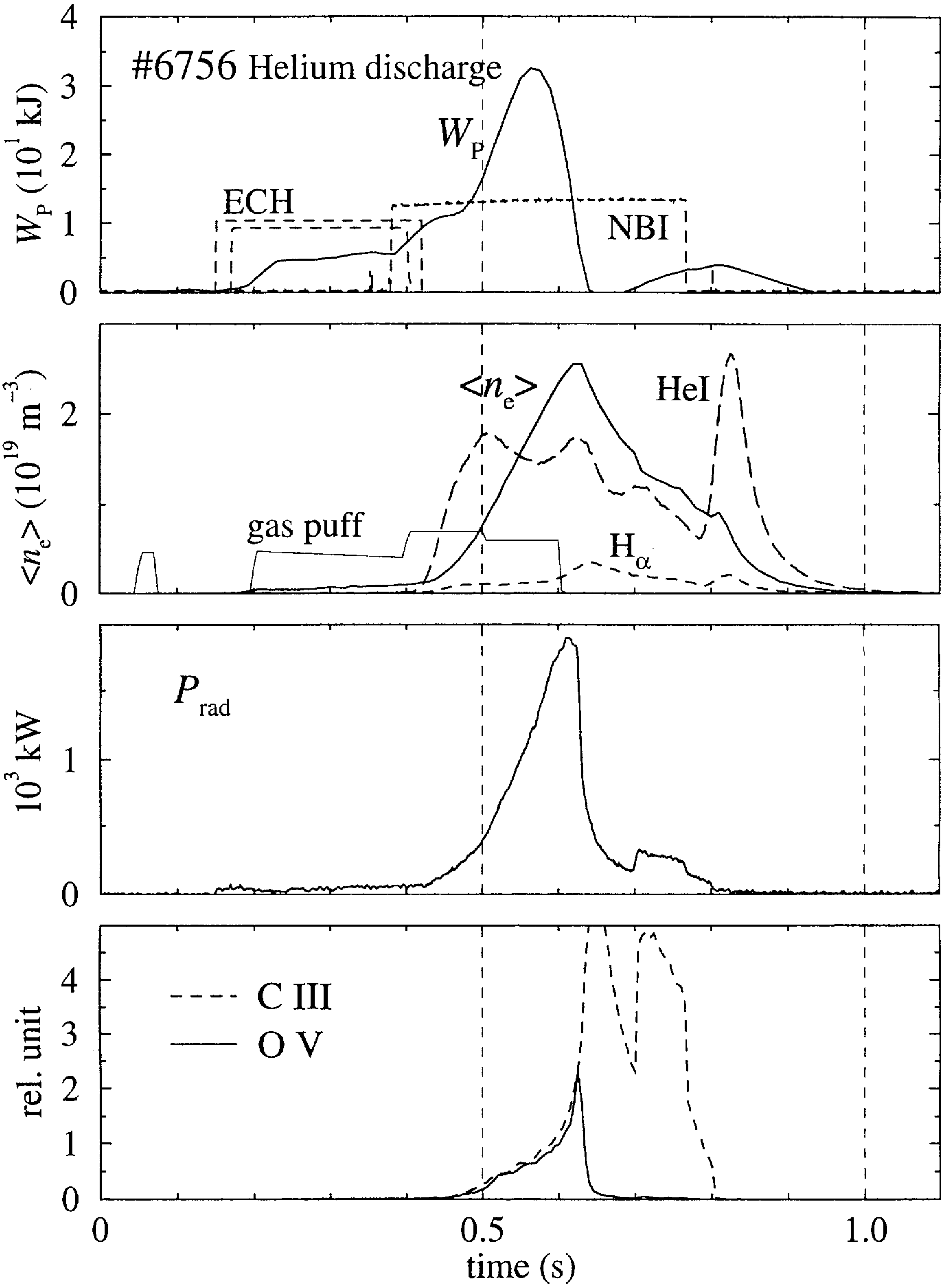

#6756 Helium discharge
W_P
ECH
NBI
W_P (10^1 kJ)
$<n_e>$
HeI
gas puff
H_α
$<n_e>$ (10^{19} m^{-3})
P_{rad}
10^3 kW
C III
O V
rel. unit
time (s)

FIG. 9

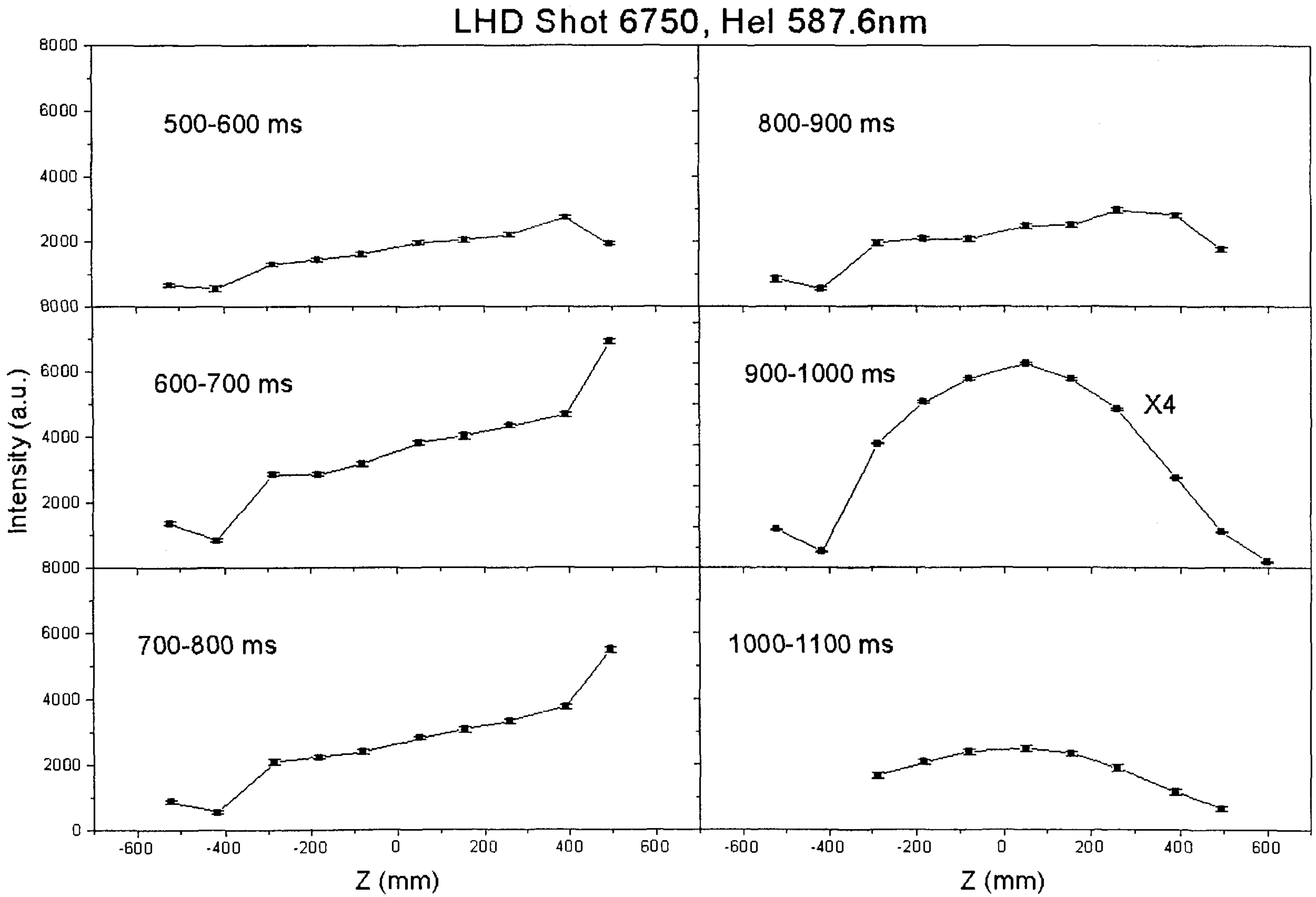

LHD Shot 6750, HeI 587.6nm
500-600 ms
800-900 ms
600-700 ms
900-1000 ms
X4
700-800 ms
1000-1100 ms
Intensity (a.u.)
0
2000
4000
6000
8000
-600
-400
-200
0
200
400
600
Z (mm)
Z (mm)

FIG. 10

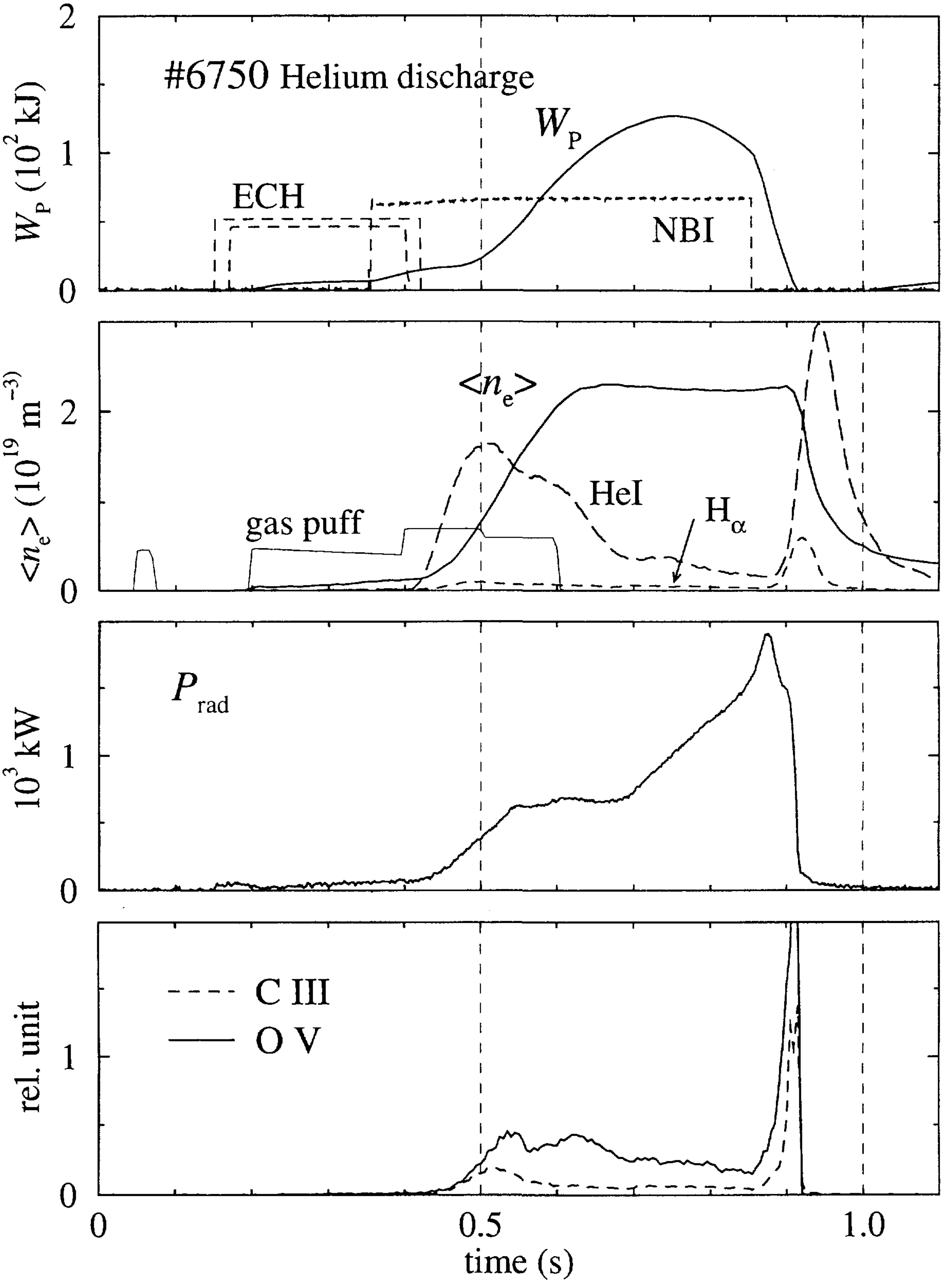
#6750 Helium discharge
W_P
ECH
NBI
W_P (10^2 kJ)
$<n_e>$
HeI
H_α
gas puff
$<n_e>$ (10^{19} m^{-3})
P_{rad}
10^3 kW
C III
O V
rel. unit
time (s)
0
0.5
1.0
2
1

FIG. 11

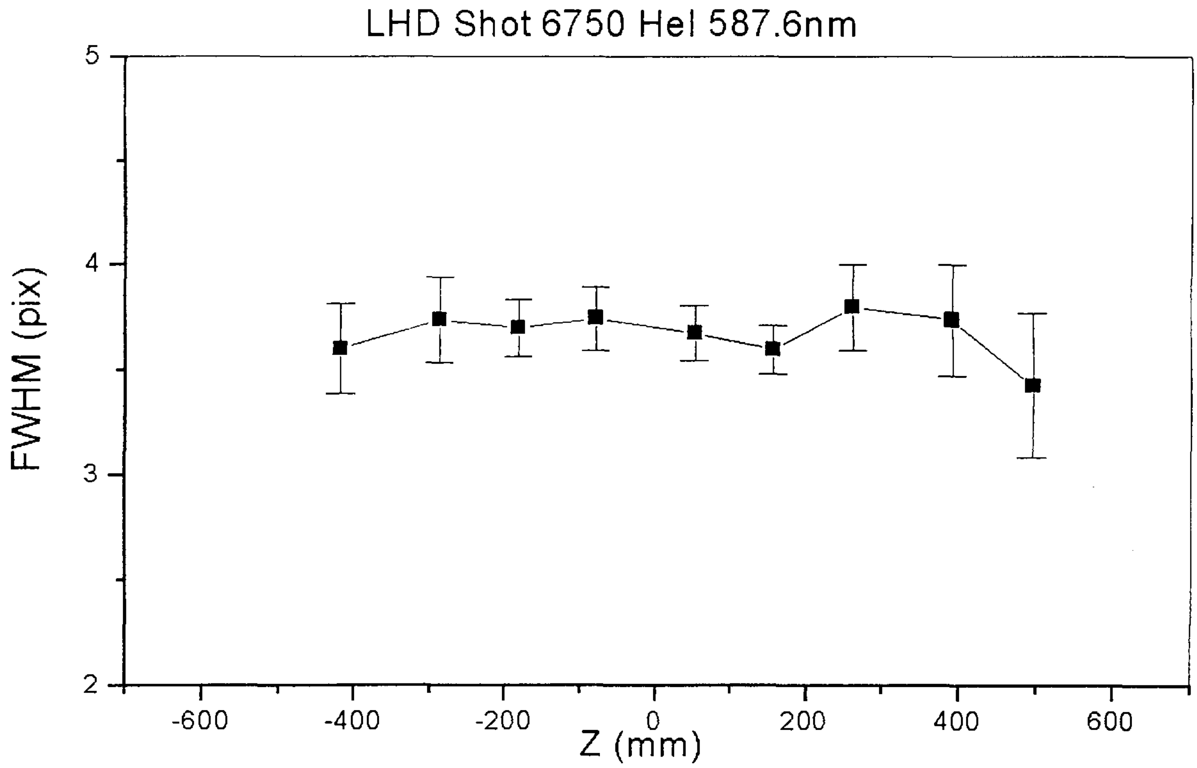

LHD Shot 6750 HeI 587.6nm
FWHM (pix)
Z (mm)

FIG. 12

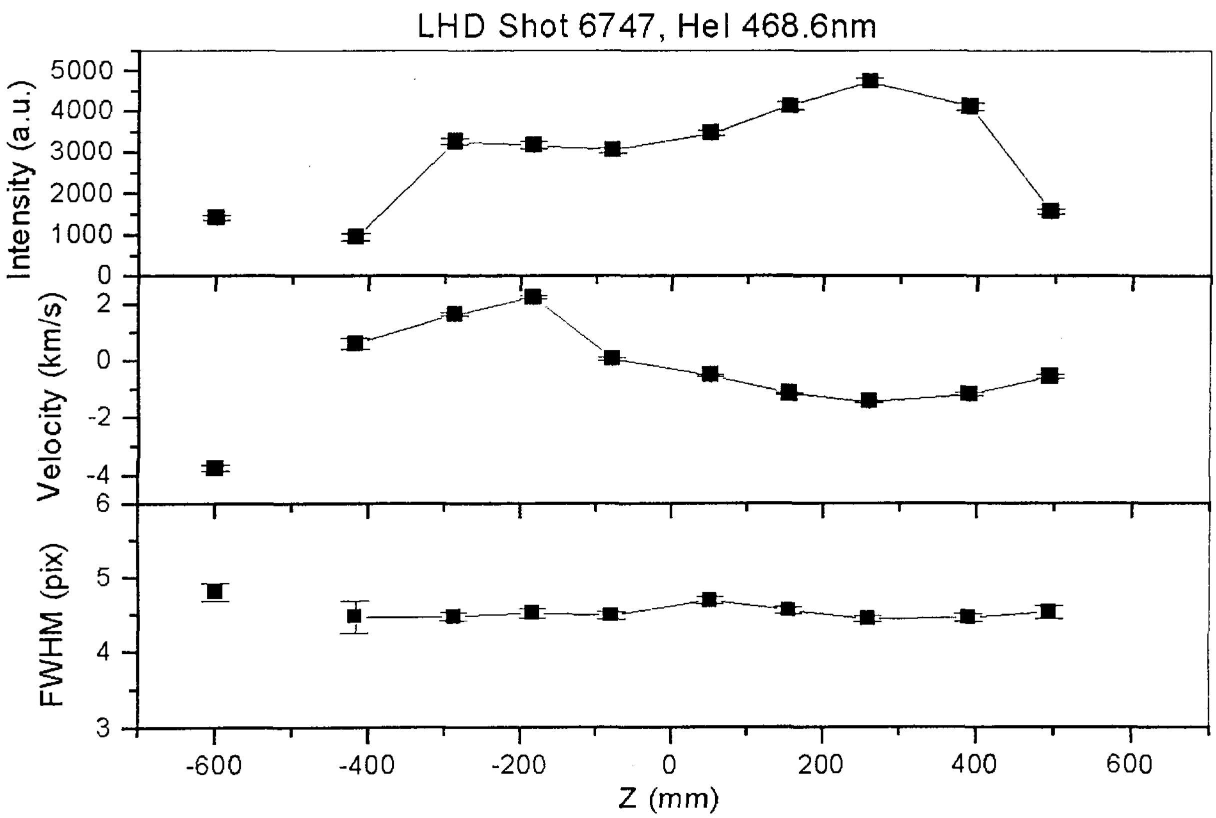

LHD Shot 6747, HeI 468.6nm
Intensity (a.u.)
Velocity (km/s)
FWHM (pix)
Z (mm)

FIG. 13

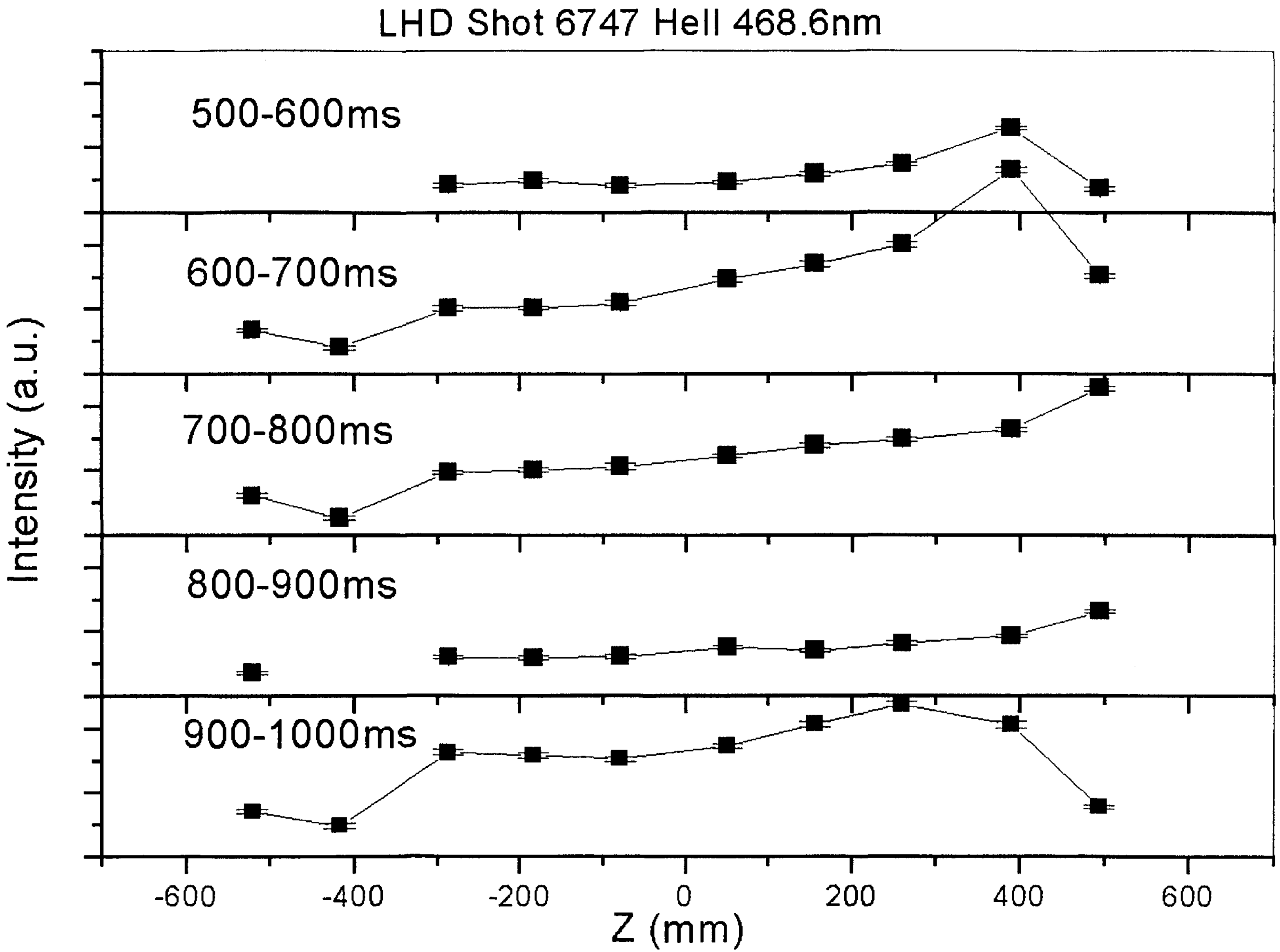
LHD Shot 6747 HeII 468.6nm
500-600ms
600-700ms
700-800ms
800-900ms
900-1000ms
Intensity (a.u.)
-600
-400
-200
0
200
400
600
Z (mm)

FIG. 14

Publication List of NIFS-TECH Series

NIFS-TECH-1 H. Bolt and A. Miyahara,
Runaway–Electron –Materials Interaction Studies ; Mar. 1990

NIFS-TECH-2 S. Tanahashi and S. Yamada,
Dynamic Analysis of Compact Helical System Power Supply and Designs of Its Upgrade; Sep. 1991

NIFS-TECH-3 J. Fujita, K. Kawahata, S. Okajima, A. Mase, T. Suzuki, R. Kuwano, K. Mizuno, T. Nozokido, J.J.Chang and C.M.Mann,
Development of High Performance Schottky Barrier Diode and its Application to Plasma Diagnostics; Oct. 1993 (in Japanese)

NIFS-TECH-4 K.V. Khlopenkov, S. Sudo, V.Yu. Sergeev,
Operation of the Lithium Pellet Injector; May 1996

NIFS-TECH-5 Nakanishi, H., Kojima, M. and Hidekuma, S.,
Distributed Processing and Network of Data Acquisition and Diagnostics Control for Large Helical Device (LHD); Nov. 1997

NIFS-TECH-6 Kojima, M., Nakanishi, H. and Hidekuma, S.,
Object-Oriented Design for LHD Data Acquisition Using Client-Server Model; Nov. 1997

NIFS-TECH-7 B.N. Wan, M. Goto and S. Morita,
Analysis of Visisble Spectral Lines in LHD Helium Discharge;June 1999